ACS Biomaterials SCIENCE & ENGINEERING

pubs.acs.org/journal/abseba

Article

Cytotoxicity of Formulated Graphene and Its Natural Rubber Nanocomposite Thin Film in Human Vaginal Epithelial Cells: An Influence of Noncovalent Interaction

Thenmozhi Sukumar, Jeslin Varghese, Kiran S, Suja Bhargavan, Parvathy Jayasree, Vemparthan Suvekbala, Kumaran Alaganandam, and Lakshminarayanan Ragupathy*

Cite This: *ACS Biomater. Sci. Eng.* 2020, 6, 2007−2019

Read Online

ACCESS | Metrics & More | Article Recommendations | Supporting Information

ABSTRACT: Graphene family materials (GFMs) are extensively explored for various biomedical applications due to their unique physical properties. The prime challenge is to establish a conclusive safety profile of these nanomaterials and their respective products or devices. Formulating GFMs with appropriate ingredients (e.g., surfactant/compatibilizer) will help to disperse them homogeneously (i.e., within the polymer matrix in the case of polymer−graphene nanocomposites) and aid in good interfacial interaction to achieve the desired properties. However, no cytotoxicity report is available on the effects of the additives on graphene and its incorporated materials. Here, we report in vitro cytotoxicity of formulated FLG (FLG-C), i.e., a mixture of FLG, melamine, and sodium poly(naphthalene sulfonate) (SPS), along with natural rubber (NR) latex and FLG-C-included NR latex nanocomposite (FLG-C-NR) thin films on human vaginal epithelial (HVE) cells. FLG-C shows reduced cellular proliferation (∼55%) only at a longer exposure time (72 h) even at a low concentration (50 μg/mL). It also displays significant down- and upregulation in mitochondrial membrane potential (MMP) and reactive oxygen species (ROS), respectively, whereas no changes are observed in lactate dehydrogenase (LDH), propidium iodide (PI), uptake, and cell cycle analysis at 48 h. In vitro experiments on NR latex and FLG-C-NR latex thin films demonstrate that the incorporation of FLG-C does not compromise the biocompatibility of the NR latex. Further substantiation from the in vivo experiments on the thin films recommends that FLG-C could be suitable to prepare a range of biocompatible rubber latex nanocomposites-based products, viz., next-generation condoms (male and female), surgical gloves, catheters, vaginal rings, bladder−rectum spacer balloon, etc.

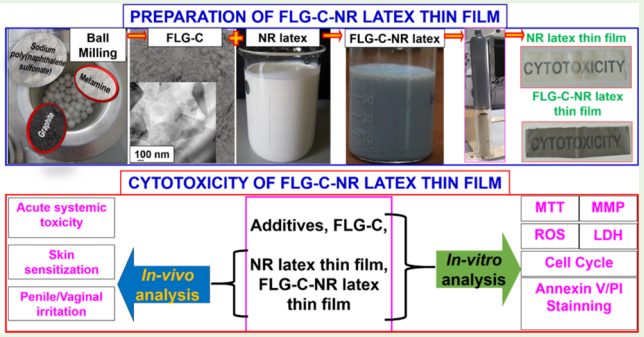

KEYWORDS: *formulated pristine few-layer graphene, graphene−natural rubber latex nanocomposites, cytotoxicity, human vaginal epithelial cells, biocompatibility*

INTRODUCTION

Because of the unique and exceptional physical properties besides the potential to tailor microstructural diversities [hydrophobic to hydrophilic and functionalized with $-NH_2$, −COOH, poly(ethylene glycol), −SH, etc.], graphene, an sp^2-hybridized two-dimensional nanomaterial, has been extensively explored for various biomedical applications, viz., biosensing,[1,2] bioimaging,[3] drug delivery,[4−6] cancer photothermal therapy,[7] and antibacterial materials.[8,9] In particular, graphene composites with different biomaterials, including polymers, have also been examined for several applications such as gloves, condoms, catheter, teeth and bone implants, scaffolds for cell culture, bioinks, etc.[10]

Numerous bottom-up (e.g., chemical vapor deposition and SiC) and top-down methods (e.g., chemical exfoliation based on Hummers' method/graphite-intercalated compounds, solvent- and/or surfactant-facilitated liquid-phase exfoliation, electrochemical expansion, and ball milling with triazine derivatives) have been established for the preparation of defect-free, monolayer to few- and multilayer graphene, graphene oxide (GO), reduced GO (rGO), as well as functionalized graphenes.[10−15] The benefits of graphene in biomaterials are: (a) increased mechanical/electrical/thermal (conductivity and stability) properties, (b) improvement of cellular attachment and growth at graphene surface, and (c) capability of loading and delivering high quantities of drugs.[16−22] In the case of graphene−polymer nanocomposites,

Received: December 12, 2019
Accepted: February 18, 2020
Published: February 20, 2020

it is possible to produce high-strength, lightweight, drug-loadable, and robust implants/medical devices.

However, the toxicity of graphene and/or graphene-based biomaterials is one of the main concerns for the prosperous product development, regulatory clearance, and its commercialization. Therefore, the interaction of graphene with different cell lines, tissues, or organs has been intensively studied and reported. Many researchers investigated the cytotoxicity of graphene to tumor cells, fibroblast cells, nerve cells, preosteoblast cells, pulmonary epithelium cells, etc.[23−29] In general, the cytotoxicity of graphene is critically associated with (a) its family members (e.g., highly hydrophobic graphene showed toxicity toward kidney epithelial cells and macrophages, and on the contrary, hydrophilic, functionalized graphene remained nontoxic),[30,31] (b) its concentrations (cell viability is decreased from substandard to 20% after exposure of GO/rGO concentrations around 10 μg/mL during 24 h or longer),[32,33] (c) its two-dimensional size [increase in the lateral size (11, 91, and 418 nm and 3.8 μm) of 2D graphene decreases (95−20%) the cell death], (d) the manufacturing methods (i.e., processing and exfoliating chemicals)[34,35] and (f) the kinds of functional groups.[36−41] In addition, researchers also observe differences in cytotoxicity with respect to different cells (HeLA cells show maximum toxicity on treatment with oxidized graphene nanoribbon compared to NIH-3T3, SKBR3, and MCF 7 due to its higher uptake of graphene).[42] Therefore, the reported investigations on the biological effects of graphene often show contradictory or inconclusive results. Consequently, it is recommended for a comprehensive material characterization and mechanistic toxicity studies for safer design and processing of each graphene to augment its respective utilization in the biomedical field. For commercial applications, GFM should be formulated with suitable additives (e.g., surfactant/compatibilizer), which helps in achieving excellent interfacial adhesion, to accomplish the most sought properties, but, no toxicity reports are available on the formulated GFM.

In our lab, we are developing a range of FLG-C-incorporated polymer nanocomposites for various personal and pharmaceutical applications.[43,44] Only a limited number of reports are available on the toxicity of FLG (i.e., produced from planetary ball milling with melamine as an exfoliating agent) using HaCat cell lines,[11,45−48] in which 80% of HaCat cell proliferation was observed with the higher concentration of FLG (100 μg/mL) at longer exposure time (72 h). However, the authors reported a significant difference in the mitochondrial membrane potential (MMP) and reactive oxygen species (ROS) even at a lower concentration (5−10 μg/mL) and a short exposure time (24 h), which could induce the cytotoxicity.[11] Herein, we report the effect of additives on the toxicity of FLG-C and its natural rubber (FLG-C-NR) latex nanocomposite thin films on HVE cells for the first time, to the best of our knowledge. In addition, the prepared thin films were also examined by in vivo experiments.

EXPERIMENTAL SECTION

Fabrication of FLG-C and NR/FLG-C-NR Latex Nanocomposite Thin Films. The detailed procedure for FLG-C preparation using planetary ball milling and latex compounding has been given in our previous reports.[43,44] In brief, ball milling was performed using graphite, melamine, and SPS (procured from Sigma) in a planetary ball mill (A Retsch PM 400) in the concentration ratio of 1:3:0.13 to obtain a formulated FLG. An aqueous dispersion of ball-milled FLG-C (30 wt %) was prepared by sonication (SONICS, 750 W) for 3 min at 25% amplitude. The graphene dispersion [1.5 (1.43) parts per 100 g of rubber (phr) (wt %)] obtained as above was incorporated into compounded NR latex [<1 wt % of nonrubber compounds (including proteins)] by sonication for 5 min. Compounding of NR latex was done with sulfur (1.5 phr—Associate Chemicals, India), activated dithiocarbamate (0.5 phr—Vanderbild), antioxidant (0.5 phr), sodium polynaphthalene sulfonate (0.037 phr—Vanderbilt), sodium salt of condensate based on naphthalene sulfonic acid and formaldehyde (0.015 phr—Chemicals and Dispersants, Mumbai), and casein (0.1 phr—Casein India) using the reported procedure.[43] Compounded NR latex and FLG-C-NR latex nanocomposite thin films were prepared using a lab model dipping machine by a two-step dipping process and vulcanized in a hot-air oven at 80 °C for 40 min. The final vulcanized samples were stripped out using silica powder and then kept at room temperature (RT; 25 °C) for 2−3 days for maturation.

Characterization of FLG-C, NR Latex, and FLG-C-NR Latex Thin Films. The thermal stability of FLG-C, NR latex, and FLG-C-NR latex thin films was calculated by thermogravimetric analysis (TGA). The samples were examined by a PerkinElmer (4000 N) under N_2 atmosphere with a heating rate of 10 °C min^{-1}. Transmission electron microscopy (TEM) was used to investigate the produced graphene dispersions (in deionized water and cell culture medium). TEM specimen was prepared by drop-casting the graphene dispersion onto a standard TEM grid. A JEOL JEM-2010 was used to analyze the samples at 200 kV. Raman analysis of FLG-C, NR latex, and FLG-C-NR latex thin films was carried out using inVia Raman imaging. A 785 nm excitation laser and 1200 l/mm grating were used. The Raman image of FLG-C-NR latex thin film was generated based on the pure reference spectra of the FLG-C using 1580 cm^{-1} as marker peak. The mapped area is >1 × 1 mm^2.

Lab-Scale Production of NR Latex and FLG-C-NR Latex Male Condom. Semi-automated lab-scale dipping machine (Plastomek, India) was employed to produce NR latex and FLG-C-NR latex male condoms (180 × 53 ± 2 mm of length and width). The process consists of (a) first dipping (glass mold) and drying, (b) second dipping and drying, (c) beading or edge rolling, (d) leaching and stripping, and (e) dehydration and vulcanization at 85−90 °C for 45 min. Then, the male condoms were kept at RT (25 °C) for 2−3 days for maturation and tested by water leaking (water leaking tester, SV Industries, India) and burst pressure and burst volume analysis (Enersol condom inflation testing equipment, Australia).

HeLA and HVE Cells Viability by [3-(4,5-Dimethylthiazol-2-yl)-2,5-diphenyltetrazolium bromide] (MTT) Assay. Initially, HeLA cells of density 5000 cells/well were taken in a 96-well plate and incubated at 37 °C in a CO_2 incubator for 24 h. Twenty microliters of FLG-C(FLG) [0(0), 50(12), 100(24), 250(60), and 500(121) μg/mL]/extracts of NR latex and FLG-C-NR latex thin film (0, 1:1, 1:2, 1:4, 1:8, and 1:16 dilution)/additives (0, 50, 100, 250, 500, and 1000 μg/mL) were added and incubated at 37 °C in the CO_2 incubator for 48 h. Then, the MTT assay on human vaginal epithelial (HVE) cells [obtained from ATCC (American Type Culture Collection), #PCS-999-003, #PCS-999-004] was conducted as described above with slight modifications, such as 4000 cells/well in 96-well plates and incubated overnight in 200 μL of media (ATCC, #PCS-480-040 and #PCS-480-030). Then, the culture supernatant was removed and 200 μL of media containing the above-mentioned concentrations of all the test materials [for FLG-C(FLG), 1000(242) μg/mL was also included] were added and incubated for 24, 48, and 72 h at 37 °C in a 5% CO_2 incubator. Similarly, cells cultured without nanomaterials were taken as control. Then, HeLA and HVE cells were incubated with MTT (20 μL; 5 mg/mL) at 37 °C for 4 h. Again, the supernatant was removed and 100 μL of dimethyl sulfoxide (DMSO) (Sigma, #D8418) was added and kept on a shaker for 20 min to dissolve the formed formazan crystals. The plates were read at 490 nm with the reference of 655 nm on a TECAN Infinite M Pro200 spectrophotometer according to the literature,[49] and cell proliferation was calculated using the formula below.

https://dx.doi.org/10.1021/acsbiomaterials.9b01897
ACS Biomater. Sci. Eng. 2020, 6, 2007−2019

$$\text{cell proliferation (\%)} = (\text{OD of the test}/\text{OD of the control}) \times 100$$

Lactate Dehydrogenase (LDH) Assay. Supernatants collected from the MTT assay on HVE cells and control (50 μL) were aliquoted in 96-well plates. LDH reagent (50 μL) was added to each well and incubated at room temperature for 15−30 min. Further, 50 μL of stop solution was added to each well and the absorbance at 450 nm was read as a main wavelength and 610 nm as the reference.

$$\text{\% of cytotoxicity} = \frac{\text{LDH released with test samples} - \text{baseline LDH}}{\text{total LDH} - \text{baseline LDH}} \times 100$$

Determination of Mitochondrial Membrane Potential (MMP), Reactive Oxygen Species (ROS), Cell Apoptosis/Necrosis and Cell Cycle Analysis. After incubation for 24 h, the HVE cells (2×10^5 cells/well in a six-well plate) were treated with the representative doses of FLG-C(FLG) [0(0), 50(12), and 250(60) μg/mL], NR latex and FLG-C-NR latex thin films (0, undiluted; 1:4, diluted), and the additives (melamine: 0, 250, and 500 μg/mL; SPS: 0, 50, and 100 μg/mL) for 48 h. Then, the treated HVE cells were trypsinized and suspended in 200 nM of 3,3′-dihexyloxacarbocyanine iodide (Thermo Scientific, #D273) in serum-free media for MMP analysis. 2′,7′-Dichlorodihydrofluorescein diacetate (Thermo Fisher Scientific, #D399) with the working concentration (5 μM) for ROS analysis and 100 μL of 1× binding buffer containing 5 μL of Annexin V-FITC and propidium iodide (PI; Abgenex, #1001 K) for apoptotic and necrotic studies were added and kept at 37 °C for 15/30 min in the dark. Centrifugation was done for 5 min and washed twice with phosphate buffer solution (3000 rpm for 2 min) and resuspended with 500 μL of serum-free media and kept in ice for MMP and ROS analyses. Whereas, 400 μL of binding buffer was added to the treated cells and filtered through a cell strainer in the case of PI staining studies. For cell cycle analysis, the cell pellets were washed with ice-cold phosphate-buffered saline (PBS) and centrifuged at 3000 rpm for 3 min. They were fixed by adding a 1 mL solution of 70% ice-cold ethanol, incubated in ice for 45 min, and again rehydrated with 1 mL of PBS and centrifuged. Cell pellet was resuspended in 100 μL of PBS containing RNase A (1 mg/mL) (Sigma, #R6513) for 30 min. Propidium iodide (10 μL, 1 mg/mL) (Sigma, #P4170) was added. Flow cytometry analyses were done using BD FACS Aria within 15 min.

Statistical Analysis. All the in vitro experiments were performed in triplicate. Student's t test was employed to acquire statistical significance.

In Vivo Experiments. Healthy adult Swiss Albino mice (weighing 17−23 g, male or female), adult New Zealand rabbits (weighing 2.6−2.7 kg, male or female), and healthy adult guinea pigs (weighing 360−470 g, male or female) were obtained from Sainath Agencies, Hyderabad, India. They were placed in stainless steel (mice and rabbits) and polypropylene (guinea pigs) cages, provided with standard laboratory diet and water ad libitum. The animal facility was maintained at 18.7−22.6 °C with a relative humidity of 37−60% for 12 h light/dark cycle throughout the experiment. These investigations were permitted by the Institutional Animal Ethics Committee [IAEC Nos. for the acute systemic toxicity (IAEC/May-2018/5 and IAEC/May-2018/6), skin sensitization (IAEC/May-2018/47 and IAEC/May-2018/48), penile irritation (IAEC/May-2018/29 and IAEC/May-2018/30), and vaginal irritation investigations (IAEC/May-2018/71 and IAEC/May-2018/72)]. These studies were executed based on the OECD Principles of Good Laboratory Practice.

In Vivo Acute Systemic Toxicity Study. In vivo acute systemic toxicity study was performed with NR latex and FLG-C-NR latex thin films using Swiss Albino mice (20 × 2 Nos.). Since the test materials cannot be administered directly to the animals, extracts of the test item (both sides) were prepared using a ratio of 6 cm^2 of the test item per mL of polar (physiological saline) and nonpolar solvents (sesame oil) at 37 ± 2 °C for 72 ± 2 h. Solvent controls were also subjected to the same temperature and time conditions. At the end of the extraction period, the appearance of the extracts was observed for change of color, turbidity, cloudy vs clear, and presence of particulate matters and is described in the Supporting Information (Table S1). The extracts were cooled to room temperature, transferred to sterile containers, and administered immediately. In each case (either NR latex or FLG-C-NR latex nanocomposites thin film), animals were divided into four sets; (i) physiological saline extract (5 Nos.), (ii) physiological saline control (5 Nos.), (iii) sesame oil extract (5 Nos.), and (iv) sesame oil control (5 Nos.). The physiological saline and sesame oil extracts (and the respective solvent controls) will be administered to the mice via intravenous (IV) and intraperitoneal (IP) routes, respectively, using sterile syringes and needles (Figure S1). Multiple doses were given (Table S2) to achieve 50 mL/kg within 24 h. However, the duration of administration shall not exceed 2 mL/min. The mice were observed and evaluated for three consecutive days for morbidity and mortality, body weight, abnormal clinical signs, and symptoms. The changes in the body weight of all of the animals were recorded (Figure S2).

Skin Sensitization Study. An in vivo skin sensitization was verified with thin films using guinea pigs (30 × 2 Nos.). Polar (physiological saline) and nonpolar (sunflower oil) extracts were prepared by extracting 6 cm^2 of thin films (of NR latex and FLG-C-NR latex thin films) per mL of solvent at 37 °C for 72 h. Animals were separated into four groups; (i) physiological saline extract (10 Nos.), (ii) physiological saline control (5 Nos.), (iii) oil extract (10 Nos.), and (iv) oil control (5 Nos.). For each phase of intradermal induction, topical application, and challenge phase, the polar and nonpolar extracts were prepared by extracting the thin films measuring 366 cm^2 (inner and outer surface) in 61 mL of physiological saline and sesame oil, respectively. Solvent controls were also subjected to the same extraction conditions. This fulfills the requirement of ISO 10993-12:2012(E).

The fur over the treatment sites was clipped and shaved on the day of treatment, prior to dosing on all the animals. Induction of sensitization was a two-stage procedure with intradermal injections on day 0 [with Freund's complete adjuvant (FCA), vehicle and extracts], followed by a topical patch exposure on day 7 for 48 h. On day 21, challenge patches were applied for 24 h (Figure S3). Skin reaction grading was performed using the Magnusson and Kligman scale (Table S3) at 24 and 48 h, after removing the challenge patches. No mortality and morbidity were observed in any of the animals used in this study. Body weight of all the animals was recorded at the start and completion of the experiments (Figure S4). No skin sensitization reactions were observed in both control and test sites of all the animals. Therefore, no gross and histopathological examinations were performed. The susceptibility of these strains of guinea pigs to a known sensitizing agent, α-hexylcinnamaldehyde (Sigma-Aldrich), has also been established as a positive control.

Penile/Vaginal Irritation Study. In vivo penile and vaginal irritation studies were performed on the thin films using New Zealand white rabbits (12 male and 12 female). The extracts of the test materials (6 cm^2/mL) were prepared using polar (physiological saline) and nonpolar solvent (sesame oil) at 37 ± 2 °C for 72 ± 2 h. Test animals free from discoloration or erythema at the test site (penile) prior to the first dose were used for the penile irritation experiment. Four groups of male rabbits, each comprising three were treated with polar and nonpolar extracts and blanks, respectively. Each animal received 0.2 mL penile application of the respective extract and blank at every 1 h for 4 h (Figure S5a). The animals were observed for two consecutive days for morbidity, mortality, signs of irritation around the penis, prepuce, and perineal area, and abnormal clinical signs and symptoms after the introduction of the sample extracts. The vaginal irritation test was performed similarly to the penile irritation test with four groups of female rabbits each comprising three rabbits. All the animals were individually restrained or the back legs were secured in such a way to expose the vagina. Before applying the extract, the catheter (6 cm short blunt) was moistened with the corresponding blank and gently inserted into the vagina, and 1 mL of extract was deposited using a syringe (Figure S5b). The animals were

https://dx.doi.org/10.1021/acsbiomaterials.9b01897
ACS Biomater. Sci. Eng. 2020, 6, 2007−2019

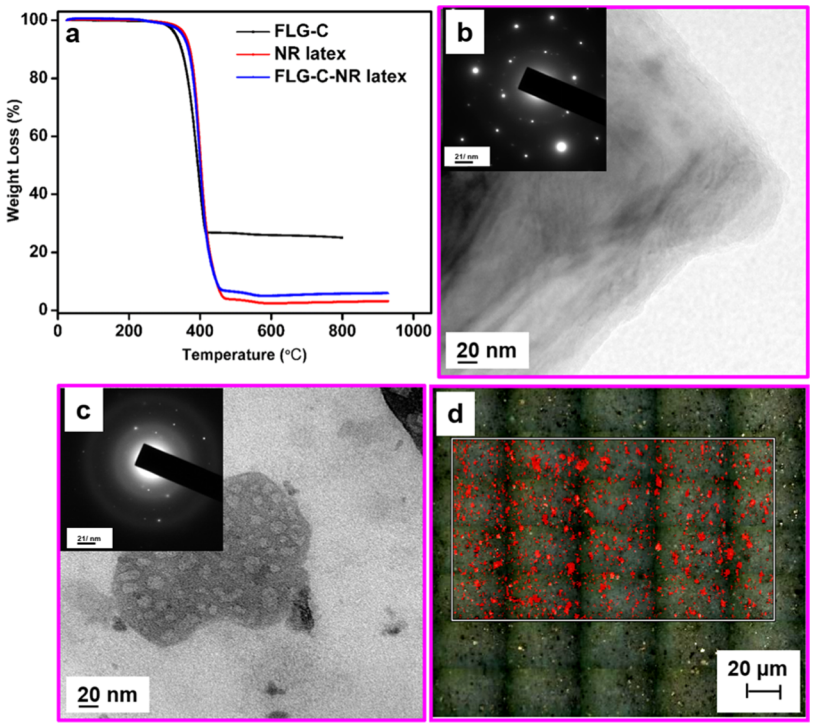

Figure 1. (a) TGA of FLG-C, NR latex, and FLG-C-NR latex thin films; (b) TEM image of FLG-C dispersed in deionized water with selected area diffraction (SAED) pattern of edge of graphene flakes; (c) TEM image of FLG-C dispersed in cell culture media with SAED; and (d) Raman image of FLG-C-NR latex thin film generating the marker peak using 1580 cm^{-1}, and the image background is made transparent to show the underlying white light image of the sample. It should be noted that not all the white light textures correspond to the Raman chemical image of the multilayer graphene.

returned to their cages after the treatment. This procedure was repeated for 5 consecutive days with a time interval of 24 h.

The animals were observed daily for general health and for external signs of irritation around the vaginal/penile opening. All the rabbits were observed and evaluated for morbidity, mortality, body weight, abnormal clinical signs, and symptoms (Figures S6 and S7). All the animals were euthanized by ketamine and xylazine injection at the end of the experiment. The entire vagina/penile was dissected and examined for the signs of irritation, injury to the epithelial layer of tissue, and necrosis. Tissues were collected and preserved in 10% buffered neutral formalin for microscopic evaluation. The tissues were subjected to dehydration procedures and processed in different grades of alcohol and washed with xylene. They were embedded in paraffin, sectioned, and stained with hematoxylin and eosin. Histopathology was carried out on the preserved organ and tissue of all the animals treated with the test items/corresponding controls. The susceptibility of New Zealand white rabbits to a known irritant, 10% sodium lauryl sulfate (positive control), and negative control (physiological saline and sesame oil) has also been carried out to confirm the validity of these experiments.

RESULTS AND DISCUSSION

Characterization of FLG-C and NR Latex/FLG-C-NR Latex Thin Films. Samples of FLG-C and NR latex/FLG-C-NR latex thin films were prepared using planetary ball milling and dip molding processes, respectively.[43] TGA of FLG-C, NR latex, and FLG-C-NR latex and TEM image of FLG-C dispersion in deionized water and cell culture medium besides Raman imaging of FLG-C-NR latex thin films are shown in Figure 1.

TGA experiments show that ∼80% weight loss was observed in FLG-C at 346 °C (Figure 1a), which is due to the decomposition of the additives (i.e., melamine and SPS)[43,44,50] adhered on the graphene surface. Both the thin films lost weight (96−98%) at the same temperature (348 °C), in good agreement with the literature.[51] A slightly lower weight (∼2%) loss was observed with the FLG-C-NR latex thin film compared to the NR latex thin film, which could be due to the presence of FLG.

Figure 1b presents the high-resolution (HR)-TEM image of FLG-C dispersed in deionized water, and it shows an overlapped flat structure with observable edges, indicating the optimum dispersion of FLG-C. To further probe the structural information of FLG-C dispersion, we present selected area diffraction (SAED) patterns, which reveal the presence of bilayer graphene with a typical hexagonal symmetry.[49] In addition, the graphene fringes corresponding to few- and multilayer graphene are also clearly visible. The size of the sheets ranges from ∼260 to 560 nm (Figure S8a,b). To characterize the degree of dispersion of FLG-C in cell culture medium and its microstructure, HR-TEM analysis was also conducted. However, the microstructures of graphene sheets including its edges are not detected due to the adhesion of proteinaceous solution and salts present in the cell culture medium (Figure 1c). Further, its SAED pattern (inset of Figure 1c) showed amorphous as well as crystalline pattern, which may be due to the adhesion of high-molecular-weight proteins, amino acids, and electron-rich ions (e.g., apo-transferin). The state of dispersion of graphene sheets within the NR latex thin film was investigated by Raman spectroscopy and imaging (Figure 1d). The FLG-C sample shows a clear G and 2D band at 1580 and 2650 cm^{-1}, respectively. Here, the shape of the 2D band indicates the presence of FLG (two to five layers).[52] The Raman spectra of NR latex and FLG-C-NR latex thin films are given in Figure S8d, in which G and 2D bands are clearly visible only for the FLG-C-NR latex thin film,

https://dx.doi.org/10.1021/acsbiomaterials.9b01897
ACS Biomater. Sci. Eng. 2020, 6, 2007−2019

Table 1. Viral Penetration Study of FLG-C-NR/NR Latex Condoms

s. no.	condom thickness (μm)	types of condoms	quantity of ϕX174 passed (μL)	burst pressure (L)	burst volume (kPa)
1	65	FLG-C-NR latex condoms	634 ± 383	44	1.6
2	75	NR latex condoms	922 ± 16	39	1.3
3	125	condoms purchased from the market	800 ± 41		

and the 2D band structure indicates the presence of multilayer graphene.[53,54] Using 1580 cm^{-1} (G band) as marker peak, the Raman image of the FLG-C-NR latex thin film is generated and shown in Figure 1d, which confirms the homogeneous distribution of multilayer graphene within the rubber matrix.

Benefits of FLG Incorporation into NR Latex. The inclusion of FLG within the NR matrix increased the tensile strength (up to 40%, without reducing the % of elongation), modulus (25%), and thermal conductivity (480−980%) compared to the NR latex thin film.[43] Tensile strength increment without reducing the % of elongation is particularly useful for the materials for skin-contacting applications (e.g., gloves, male/female condoms).

Evaluation of FLG-C-Incorporated NR Latex Male Condoms. To prove the nanocomposite thin film application, FLG-C-NR latex male condoms were produced by the dip molding process. To test the optimum penetration properties of the materials (as a condom) in serous fluids, burst pressure (BP), burst volume (BV), water leakage, and viral penetration studies were performed according to the ISO 4074-2015 (i.e., the condoms must have the minimum burst pressure of 1 kPa and burst volume of 16 L). Our experiments clearly demonstrate that FLG incorporation into NR latex has increased the BP and BV compared to the control condoms. No water leaking was observed in the FLG-C-NR latex condoms as similar to NR latex condoms.

We have also assessed the capability of the FLG-C-NR latex condom as an effective barrier against viruses (e.g., HIV; 100−110 nm, HBV; 47 nm), a viral penetration test (shown in Supporting Information Figure S9)[55] as completed for FLG-C-NR latex condoms with the necessary controls [conventional condom (without FLG-C) and conventional condom available in the market (control for brand comparison)] using bacteriophage ϕX174; 26 nm in size (ATCC 13706-B1) and *Escherichia coli* strain C (ATCC 13706). The quantity of ϕX174, which passes through the FLG-C-NR latex condom was calculated (Plague Forming Unit/mL) by plague forming assay (PFA). The limit of detection of PFA and the loss of ϕX174 during the experiment were all also calculated and accounted as a correction factor. The results (Table 1) show that FLG-C-NR latex condoms have a similar viral passage to the currently existing condoms. However, the viral penetration level is observed to be higher compared to the literature (0.1−200 μL).[55] The observed higher amount of ϕX174 diffusion in our experiments may be due to the fact that the loss of ϕX174 during the experiment was included as penetrated.

MTT Assay on HeLA and HVE Cells with FLG-C and NR Latex/FLG-C-NR Thin Films. FLG-C and the extracts of NR latex and FLG-C-NR latex nanocomposite thin films show no toxicity in HeLA cells (Figure S10a−c) even at their highest concentration [>80% viability with 500(121) μg/mL of FLG-C(FLG) and the undiluted extracts of the thin films]. In comparison, Luo et al.[56] showed a slightly reduced proliferation on HeLA cells (~70% viability at 100 μg/mL) with pyrogallol-stabilized rGO. This small difference in HeLA cell proliferation with FLG and rGO may be due to the remaining oxygen functionalities at rGO. However, melamine and SPS show a small reduction in cellular proliferation (~75% viability at 1000 μg/mL) at 48 h.

Similar MTT assays were also performed on HVE cells. >80% of the HVE cells were viable at 24 and 48 h exposure of FLG-C even at the highest concentration (1000 μg/mL). However, ca. 40−50% of cell death was observed at 72 h even with the lowest concentration of FLG-C (50 μg/mL). Pelin et al.[11] also reported a similar toxicity level of FLG in HaCat cells (e.g., ~76% of viability to 10 μg/mL of FLG at 72 h). In contrast, the extracts of NR latex and FLG-C-NR latex thin films show no toxicity even with the highest concentration (undiluted) and longer exposure time (72 h). However, melamine shows a moderate decrease in HVE cell proliferation (~62% viability at 500 μg/mL and 48 h), whereas the surfactant SPS displays a severe decrease in the cell propagation with respect to dose and exposure time (<10% viability at 500 μg/mL and 48 h) (Figure S10d). Melamine is scarcely soluble in water due to its intermolecular H-bonding (only soluble in water at 60−70 °C), which may due to its relatively lesser toxicity compared to the surfactant.

It is remarkable to observe that at 48 h, the highest dose of FLG-C (1000 μg/mL), which contains 242, 726, and 30 μg/mL of FLG, melamine, and SPS, respectively, is not reducing the viability of HVE cells (>80%). At the same time, even the lowest investigated amount of FLG-C (50 μg/mL) that includes 12, 36, and 1.6 μg/mL of the same compounds as above is decreased the HVE cell viability to ~60% at 72 h. FLG and the additives form a complex through noncovalent interactions ($\pi-\pi$ and H-bonding); therefore, the individuals may not be freely available for the cellular uptake. However, this complex is radically getting disturbed at longer exposure time (72 h) and decreases the cellular proliferation significantly even at the lowest dose of the FLG-C.

Interestingly, the FLG-C-NR latex thin film shows no toxicity with respect to dose and exposure time similar to the NR latex thin film. It is due to the fact that homogeneous dispersion of FLG-C within the rubber matrix does not allow the FLG-C to leach into the cell culture medium during the extraction. It is well known that the production method plays a key role in the cytotoxicity of material. FLG can be prepared using a number of methods such as chemical exfoliation using ball milling, liquid-phase shear exfoliation, arc discharge method, etc. For example, a report by Sasidharan et al.[45] shows that FLG obtained by the arc discharge method has cytotoxicity (<10% viable) on human umbilical vein endothelial cells with 10 μg/mL at the exposure time of 24 h. In contrast, FLG (100 and μg/mL)[11] and FLG-C (1000 μg/mL) prepared by planetary ball milling are not affecting the cellular viability on HaCat and HVE cell lines, respectively, at 24 h.

An examination of cell morphology using optical microscopy exhibited that the effects witnessed in all of the treated groups were comparable. Representative optical images of the cells after treatment with FLG-C, NR latex, and FLG-C-NR latex thin films are shown in Figure 2, while the remaining images

https://dx.doi.org/10.1021/acsbiomaterials.9b01897
ACS Biomater. Sci. Eng. 2020, 6, 2007−2019

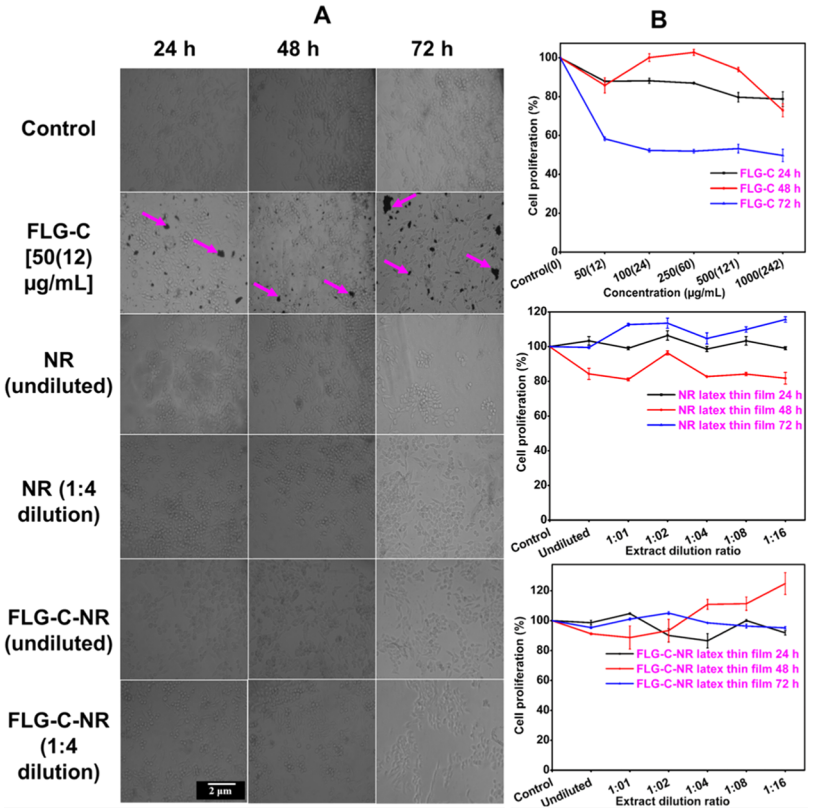

Figure 2. (A) Optical images (10× scale, 2 μm) and (B) cell proliferation (by MTT assay) of HVE cells after treatment with FLG-C (FLG), NR latex thin film, and FLG-C-NR latex thin film. The arrows indicate the presence of FLG.

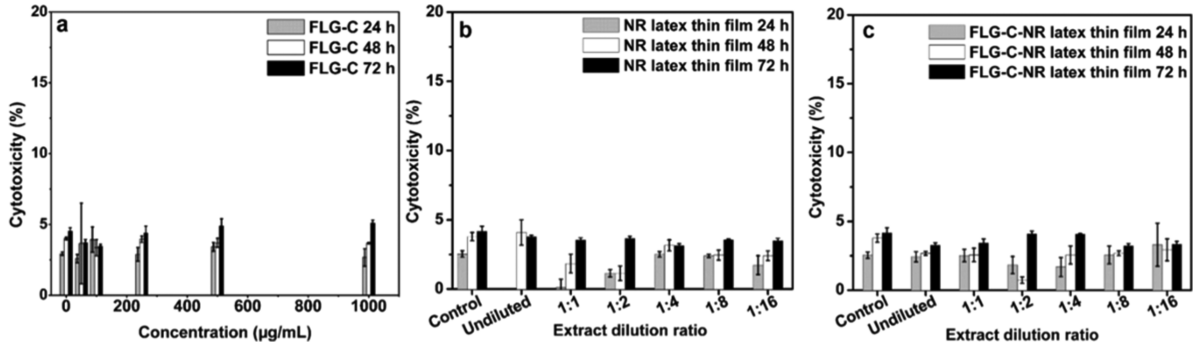

Figure 3. LDH release after treatment with (a) FLG-C ($p < 0.5$), (b) NR latex thin film ($p < 0.2$), and (c) FLG-C-NR latex thin film ($p < 0.5$) in 24, 48, and 72 h.

are given in the Supporting Information (Figures S11 and S12). In the case of FLG-C, the increased concentration of FLG is notified as block spots in the given optical images. Nevertheless, the cell membrane integrity was not affected by all the investigated materials.

LDH Assay on HVE Cells with FLG-C and NR/FLG-C-NR Latex Thin Films. The interaction or accumulation of the tested materials on the HVE cells after treatment was investigated with the LDH assay. It should be noted that LDH release is due to the cell membrane damage, which leads to cell death. During the above MTT assay with HVE cells, the supernatants (cell culture medium) were separated and subjected to the LDH assay. Neither dose- nor time-dependent LDH release is observed in all the cases (except surfactant). This indicates that all the investigated samples preserve the plasma membrane integrity; hence, there is no cytotoxicity in HVE cells (Figure 3). The surfactant shows a dose-dependent LDH release; however, the quantified LDH amount is of only a small extent upward (Figure S13). As discussed earlier, the MTT assay clearly indicates a significant decrease in cell viability for FLG-C and a dose-dependent toxicity for melamine and surfactant at 72 h. The disagreement between the MTT and LDH assays (especially at 72 h) suggests that the vaginal cell death may be due to the mitochondrial membrane disintegration, not because of the cell membrane damage.

Effects of FLG-C and NR Latex/FLG-C-NR Latex Thin Films on MMP and ROS Production. During ATP synthesis through oxidative phosphorylation in mitochondria, the electron transport chain creates an electrochemical gradient and generates MMP. A substantial loss of $\Delta\Psi_m$ causes loss of energy and leads to death. Representative doses of the test materials were evaluated by means of mitochondrial depolarization after 48 h. A minor reduction in MMP (i.e., 1.7−3.3%) was observed with FLG-C, NR latex, FLG-C-NR latex thin

https://dx.doi.org/10.1021/acsbiomaterials.9b01897
ACS Biomater. Sci. Eng. 2020, 6, 2007−2019

films (Figure 4a), and melamine with respect to the negative control (4.7%, Figure S14a), whereas the surfactant showed a

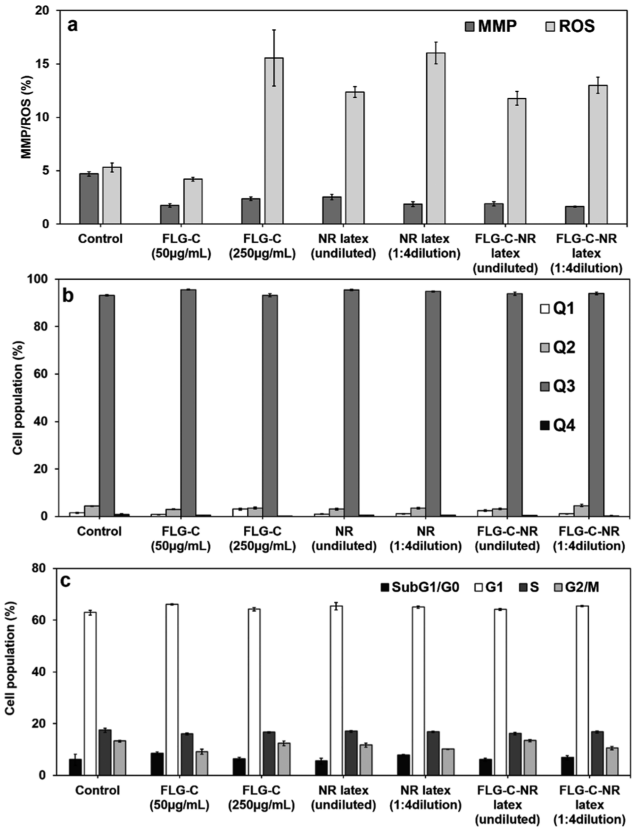

Figure 4. (a) MMP ($p < 0.027$)/ROS ($p < 0.22$), (b) PI uptake ($p < 0.15$), and (c) cell cycle analysis ($p < 0.5$) of HVE cells after treatment (48 h) with representative concentrations of FLG-C and extracts of NR latex and FLG-C-NR thin films.

significant loss of MMP (0.3%) compared to the negative control. However, these observed changes on MMP at 48 h for all the treated materials were not affecting the HVE cell proliferation.

ROS are reactive molecules and free radicals derived from molecular oxygen. High levels of ROS can lead to cellular damage, oxidative stress, and DNA damage and elicit either cell survival or apoptosis mechanisms. The above MMP experiments indicate that there is a minor to significant loss of MMP with the tested materials. Hence, we further investigated ROS production in the HVE cells after treatment of the same representative doses of the materials at 48 h. FLG-C (50 μg/mL) and the negative control (cells not exposed to FLG-C) show a similar ROS release pattern, i.e., 4.2 and 5.3%, respectively (Figure 4a). However, increasing the FLG-C content to 250 μg/mL displayed a rise in ROS release, i.e., 17.4%. This is in good agreement with the reported ROS production (18.5%) with 100 μg/mL of FLG on HaCat cells.[48] The elevation in ROS production in the case of FLG-C may be due to the valence electron (in graphene), which is ready to localize on the edges or defects. This endows them with highly reactive free radical.[57] One of the additives, melamine, does not show any significant increase in the ROS value (3.1 and 6.0% of ROS for 50 and 250 μg/mL of melamine, respectively) compared to the negative control. At the same time, the surfactant releases a dose-dependent ROS (i.e., 40 and 58% of ROS with the doses of 50 and 100 μg/mL, respectively) (Figure S14a), however not affecting the HVE cell proliferation. Impressively, both NR latex and FLG-C incorporated NR latex thin film extracts show similar levels of ROS production (11.1−15.6%) (Figure 4a) and do not show any dose dependency, which suggests that the leachables from both the materials may be identical (in terms of quality and quantity). Surprisingly, the % ROS released for melamine is observed to be similar compared to the negative control that may be due to the intermolecular H-bonding (reduces its solubility in water at room temperature). The surfactant shows a dose-dependent ROS release (Figure S14a), however not influencing the viability of HVE cells. All these results are in line with our MTT results obtained at 48 h.

Cell Apoptosis/Necrosis and Cell Cycle Analysis. Annexin V/propidium iodide assay and cell cycle analysis were performed to quantify necrotic, apoptotic and live cells and to understand the cell division process after treatment with test materials, respectively. Figure 4b demonstrates that the test materials treated with HVE cells mostly accumulate (≥93%) in live cell quadrant Q3. However, a minor proportion of necrotic (0.6−4%) and late apoptotic (3.2−4.8%) cells was also observed in all the cases. Similarly, melamine and SPS showed more cells on Q3 and very limited % of cells observed in Q2 (Figure S14b). These results also support the previous findings of the LDH assay, i.e., cell death is not due to the plasma membrane damage. Similarly, Pelin et al.[11] reported significant PI uptake (∼60%) with 100 μg/mL FLG on HaCat cells at 48 h; however, it did not decrease the cellular proliferation. In contrast, the current investigation shows a good agreement between the cell proliferation (MTT assay) and the PI uptake at 48 h for FLG-C and the extracts of NR latex and FLG-C-NR latex thin films. The additives also do not show a significant amount of PI uptake at 48 h (melamine: 250 μg/mL and SPS: 100 μg/mL) in good agreement with the MTT assay.

The above results clearly indicate that FLG-C and NR latex/FLG-C latex thin films and the additives are limited/no cell death but significant cellular uptake may be possible in all of the cases. Hence, we conducted a fluorescence-activated cell sorting (FACS)-based cell cycle analysis, which provides information about % of cells in each phase of the cell cycle (G0/G1, S, and G2/M). As shown in Figures 4c and S14c, the cells exposed to the investigated materials induced a substantial accumulation of cells in the G0/G1 phase. These results indicate that the studied materials are not showing a significant impact in the cell cycle process, in good agreement with the other experimental data.

Summing up, FLG-C shows no cytotoxicity up to 48 h with the highest concentration. However, on longer exposure time (72 h), it induces cytotoxicity even at the lowest concentration (50 μg/mL). No significant amount of LDH release is observed in all these cases. These results suggest that the reduced cellular proliferation (predicted by MTT assay) could be due to the mitochondrial membrane damage. Furthermore, FLG-C shows a decrease and increase in the MMP and ROS production, respectively, at 48 h. PI uptake and cell cycle analysis experiments on FLG-C are not showing noteworthy difference with respect to the negative control at 48 h. At the same time, the extracts of NR latex and FLG-C-NR latex thin films do not affect the mitochondrial and plasma membranes; hence, no toxicity appears to be induced.

https://dx.doi.org/10.1021/acsbiomaterials.9b01897
ACS Biomater. Sci. Eng. 2020, 6, 2007−2019

Table 2. Comparison between Reported Works on Toxicity of FLG and the Current Work

			in vitro cytotoxicity			
FLG or GO	production method or purchased sample	I_D/I_G ratio	cell line and assays	dose (μg/mL) and exposure time	Is product fabricated and tested?	ref
FLG	ball milling	0.2	HaCat and WST-8, SRB, PI staining	0.005−90 (FLG)/0.005−100 (GO1-3) and 24/48/72 h and 10 days	no	11
GO1-3	purchased	broad				
FLG	ball milling	0.35	HaCaT and NMR-based metabolomics, cell apoptosis, necrosis, and viability and determination of $O_2^{\bullet-}$, H_2O_2, and Ca^{2+}	0.5−200 and 24/48 h and 7 days.	no	47
GO	purchased	0.94				
FLG	ball milling	0.4	HaCaT MMP, ROS, and cell viability	1−100 and 24/72 h	no	48
GO	purchased	<1				
FLG	arc discharge	–	human primary endothelial cells	0−10 and 24 h	no	45
FLG	purchased	0.51	RAW 264.7	2.5−40 and 24 h	no	46
FLG-C	ball milling	0.41−0.49	HVE and HeLA cells and MTT, MMP, ROS, LDH, annexin staining, and cell cycle analysis	0−1000 and 24/48/72 h	yes	current work
NR latex	dip molding	–	the same above in vitro in HVE and HeLA cells plus in vivo investigations	0 to undiluted to 1:16 dilution	yes	current work
FLG-C-NR latex	dip molding	–	the same above in vitro and in vivo experiments	0 to undiluted to 1:16 dilution	yes	current work

Table 3. Clinical Observation of the Animals Treated with NR Latex and FLG-C-NR Latex Thin Films in Acute Systemic Toxicity[a]

Sample	Group No.	Animal No.	Sex	Observation at (h) 0	0.5	4	24	48	72
NR latex thin film	G1	1, 2, 3, 4 and 5	M	Normal					
	G2	6, 7, 8, 9 and 10	M	Normal					
	G3	11, 12, 13, 14 and 15	M	Normal					
	G4	16, 17, 18, 19 and 20	M	Normal					
FLG-C-NR latex thin film	G1	1, 2, 3, 4 and 5	F	Normal					
	G2	6, 7, 8, 9 and 10	F	Normal					
	G3	11, 12, 13, 14 and 15	F	Normal					
	G4	16, 17, 18, 19 and 20	F	Normal					

[a]M—male; F—female; G1 and G3—physiological saline and sesame oil control; and G2 and G4—physiological saline and sesame oil extract of the samples.

Akhavan et al.[58] reported the cytotoxicity of rGO of different lateral size dimensions (11 ± 4, 91 ± 37, and 418 ± 56 nm) and as-prepared GO (3.8 ± 0.4 μm) with human mesenchymal stem cells. The study clearly indicates a significant size-dependent cytotoxicity, i.e., a treatment concentration of 100 μg/mL of rGO (11 ± 4 nm) showed >95% cell death while the increasing sizes (418 ± 56 nm) of rGO reduces the cell death (~60%) significantly. At the same time, the prepared GO with largest lateral size dimensions (3.8 ± 0.4 μm) showed the lowest (~30%) cytotoxic influence. In our investigations, the observed biocompatibility of FLG-C up to 48 h is due to the facts that: (a) the investigated FLG has a higher lateral dimension, i.e., ca. 260−560 nm, (b) melamine is having very strong (noncovalent) $\pi-\pi$ interaction with the FLG[54] and may not be freely available for the cellular uptake, and (c) the quantity of the other additive (i.e., surfactant) is very less (i.e., 0.13 wt %). On the other hand, the toxic additives used for rubber compounding, such as sulfur, ZnO, ZMPT, etc., and FLG-C are completely integrated (through covalent and noncovalent bonds) with the NR matrix and may not leach into the cell culture medium at 37 °C. Therefore, the extracts of the thin films do not exhibit cytotoxicity to both HeLA and HVE cells.

A comparison between the reported toxicity studies on FLG with the current work is given in Table 2. It appears that the formulation of FLG with melamine and SPS increases the biocompatibility. In addition, the plausible application of FLG-C with NR latex thin film is established and proved their biocompatibility in HeLA and HVE cells. However, to get a conclusive cytotoxicity data, the following in vivo experiments were also performed on NR latex and FLG-C-NR latex thin films.

In Vivo Acute Systemic Toxicity of NR Latex and FLG-C-NR Latex Thin Films. Acute systemic toxicity provides general information on health hazards likely to arise from acute exposure by an intended clinical route. The evaluation includes the presence/absence and incidence and severity of abnormalities, including behavioral and clinical abnormalities, gross

https://dx.doi.org/10.1021/acsbiomaterials.9b01897
ACS Biomater. Sci. Eng. 2020, 6, 2007−2019

lesions, body weight changes, effects on mortality, and any other general or specific effects. The acute systemic toxicity potential of the thin films was evaluated in male Swiss Albino mice. The first two groups (G1 and G2) were treated intravenously with polar extracts of the thin films and solvent control, respectively. The other two groups (G3 and G4) were treated intraperitoneally with nonpolar extracts of the thin films and nonpolar solvent control (Table S2) accordingly. The control solvent-administrated animals (G2 and G4) did not show any significant loss in body weight as well as any mortality or abnormal behavior. Similarly, sample extracts administrated animals (G1 and G3) showed no mortality or morbidity. However, all animals in the groups showed a very slight increase of about 0.5 g in body weight after 72 h (Figure S2). We found nil signs of clinical toxicity or overt toxicity in any of the animals (Table 3), and hence gross pathology and histopathology were not performed. Therefore, the observed results suggest that both the extracts of NR latex and FLG-C-NR latex thin films did not show any systemic toxicity.

In Vivo Skin Sensitization Test. To assess the biocompatibility of medical devices, sensitization (type IV hypersensitivity reaction) is a key toxicity endpoint. We determined the skin sensitization potential of the thin films using guinea pig maximization test. Skin sensitization of the sample extracts and the solvent controls were studied to compare their biological responses. Table S4 shows the skin sensitization of a positive control α-hexylcinnamaldehyde, which demonstrated (grading of 1−2) discrete or patchy erythema to moderate and confluent erythema.

Grading of skin reactions performed at 24 and 48 h after removing the challenge patch is presented in Table 4. No mortality and morbidity in any of the animals tested with either NR latex or FLG-C-NR latex thin film extracts were observed. Furthermore, there is no skin reaction elicited in terms of incidence and severity between both control (G1 and G3) and sample (G2 and G4) groups. All the animals showed an increase in body weight at the end of the experiment (Figure S4). No skin reactions occurred in any of the sample extract-treated animals and proved no sign of sensitization. These results confirmed that the FLG-C-NR latex thin film nanocomposite is a safe material for skin-contacting applications similar to the NR latex thin film.

Table 4. Grading of Skin Sensitization Reaction on Guinea Pigs after Removal of the Challenge Patch[a]

				Magnusson and Kligman scale			
				24 h		48 h	
sample	group	sex	animal no.	C	T	C	T
NR latex thin film	G1	M	1, 2, 3, 4, and 5	0	0	0	0
	G2	M	6, 7, 8, 9, 10, 11, 12, 13, 14, and 15	0	0	0	0
	G3	M	16, 17, 18, 19, and 20	0	0	0	0
	G4	M	21, 22, 23, 24, 25, 26, 27, 28, 29, and 30	0	0	0	0
FLG-C-NR latex thin film	G1	F	1, 2, 3, 4, and 5	0	0	0	0
	G2	F	6, 7, 8, 9, 10, 11, 12, 13, 14, and 15	0	0	0	0
	G3	F	16, 17, 18, 19, and 20	0	0	0	0
	G4	F	21, 22, 23, 24, 25, 26, 27, 28, 29, and 30	0	0	0	0

[a]M—male; F—female; G1 and G3—physiological saline and sesame oil control; and G2 and G4—physiological saline and sesame oil extract of the samples. C and T are the control and test sites, respectively.

Penile Irritation using New Zealand White Rabbits. Penile irritation study is one of the endpoints to assess the biocompatibility of medical devices, which comes in contact with penile tissue, e.g., condom, catheter, surgical gloves, etc. This is a sensitive method to assess the irritation potential of the sample to the penile tissue. In this test, we examined the penile (mucosal membrane) irritation potential of the thin film extracts on New Zealand white rabbits. During the experiment, no clinical signs of ill health or overt toxicity were observed in any of the treated animals. However, all the animals showed an increase in body weight at the end of the experiment (Figure S6). Further, they were euthanized at 48 h following the final dosage. The penile tissue dissected from the animals was examined for the macroscopic and microscopic signs of irritation. No evidence of irritation was observed in the penile mucous membrane. Observations were graded according to the numerical scale for both the test items and the corresponding controls (Tables S5 and S6). None of the animals exhibited redness at the penile tissue prior to the initial application. Furthermore, no gross or histopathological lesions were observed in the penile tissue after treatment with the test items. The entire penis and sheath was dissected and examined macroscopically for the signs of irritation. The tissues were then embedded in paraffin, sectioned, and stained with hematoxylin and eosin.

Tables 5 and S7 show the average grades of gross pathology and histopathological evaluation, respectively, for all the animals treated with the sample extracts and solvent controls. In gross pathology, no abnormalities were observed in all the investigated animals. Microscopic images of stained penile tissues are illustrated in Figure 5. Saline and oil controls show a normal penile submucosa in both 10× (a, e, i, m) and 40× (b, f, j, n) magnification. Penile tissues treated with the thin film extracts [NR thin film extracts in saline (c) & (d) and oil (g) & (h), respectively, whereas FLG-C-NR thin film extract in saline (k) & (l) and oil (o) & (p), respectively] also confirm the standard penile submucosa. The images were interpreted using histopathology grading system. Here, the average difference between the test item, i.e., animals treated with extracts of the thin films, and the solvent controls was within the acceptable limits. It demonstrates (Tables S7 and S8) that the penile submucosa is having minimal (grade 1) vascular congestion after treatment with the thin film extracts. The positive and negative control experiments show moderate irritant (grade 3) and nonirritant (grade 0) reactions, respectively, confirming the validity of this experiment.

Table 5. Gross Pathology Examination of Penile Tissue Reactions with the Thin Film Extracts

	group	animal no.	macroscopic evaluation
NR latex thin film	G1	1, 2, and 3	no abnormality was detected
	G2	4, 5, and 6	
	G3	7, 8, and 9	
	G4	10, 11, and 12	
FLG-C-NR latex thin film	G1	1, 2, and 3	no abnormality was detected
	G2	4, 5, and 6	
	G3	7, 8, and 9	
	G4	10, 11, and 12	

https://dx.doi.org/10.1021/acsbiomaterials.9b01897
ACS Biomater. Sci. Eng. 2020, 6, 2007−2019

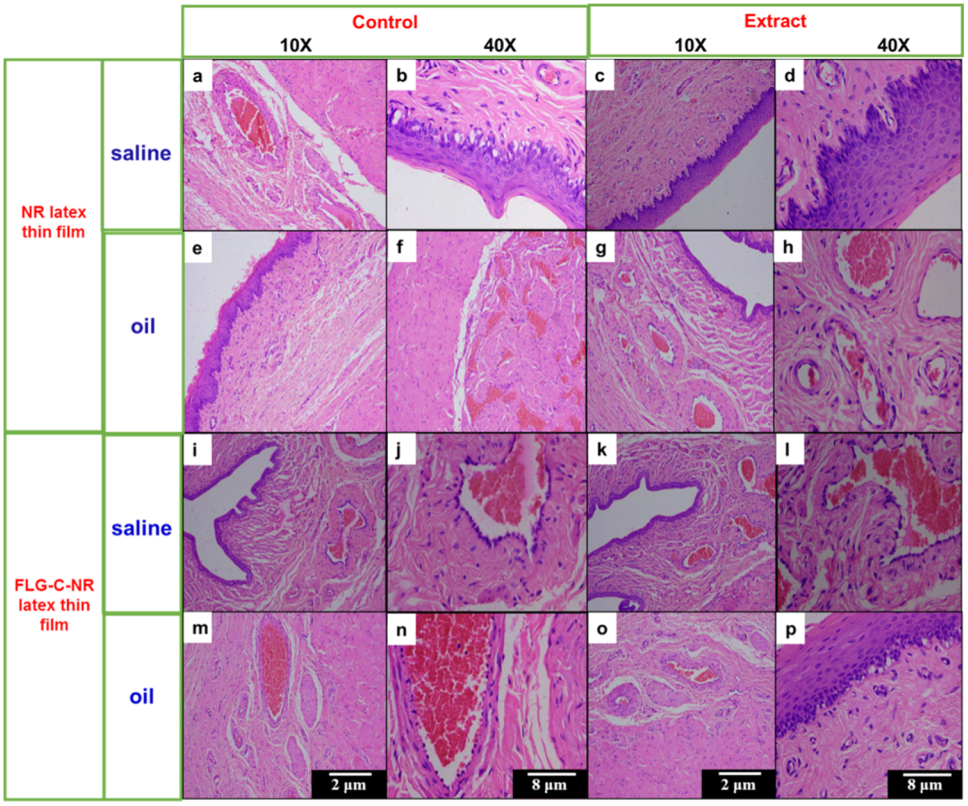

Figure 5. Representative hematoxylin and eosin-stained histopathology images of penile tissues of New Zealand white rabbits.

Vaginal Irritation Test. Vaginal irritation potential of the thin films was evaluated in female (nulliparous and non-pregnant) New Zealand white rabbits. As discussed in the penile irritation study, this test is also important to assess the biocompatibility of the medical devices that come in contact with vaginal tissues. No clinical signs of ill health or overt toxicity were observed in any of the treated animals. All the animals were euthanized after the final treatment of extracts (fifth day). The entire vagina was dissected and examined for any macroscopic and microscopic lesions. Furthermore, no gross or histopathological lesions related to treatment with test item (extracts) were observed. Tissues were embedded in paraffin, sectioned, and stained with hematoxylin and eosin.

Tables 6 and S9 represent the average grades of gross pathology and histopathological evaluation, respectively, for all of the animals treated. Similar to the penile irritation investigation, here also no abnormalities were observed in gross pathology investigation of the vaginal tissues treated with the test items and controls. Microscopic images of stained vaginal tissues are shown in Figure 6, which represents the histopathology images of control [a, b, i, and j (saline) & e, f, m, and n (oil)], NR latex [c and d (saline extract) & g and h (oil extract)], and FLG-C-NR latex [k and l (saline extract) & o and p (oil extract)] thin film-treated vaginal tissues. All the tissues were graded according to the grading system for microscopic examination of vaginal tissues. The vaginal tissue after treatment showed minimal or mild leukocyte infiltration that proves no manifestations of abnormalities. The average scores were within the acceptable limits (grades 1−2) (Table S10), and it is proven that the FLG-C-incorporated NR latex thin film is nonirritant (Table S11) to vaginal mucous membrane of the rabbits.

Table 6. Gross Pathology Examination of Vaginal Tissue Reactions

sample	group	animal no.	macroscopic evaluation
NR latex thin film	G1	1, 2, and 3	no abnormality was detected
	G2	4, 5, and 6	
	G3	7, 8, and 9	
	G4	10, 11, and 12	
FLG-C-NR latex thin film	G1	1, 2, and 3	no abnormality was detected
	G2	4, 5, and 6	
	G3	7, 8, and 9	
	G4	10, 11, and 12	

For all the in vivo experiments, either physiological saline or sunflower/sesame oil extracts of the thin films were employed. Physiological saline cannot deteriorate the natural rubber, and leaching of toxic ingredients (except the water-soluble proteins, which is in the natural rubber) may not be possible. At the same time, sunflower/sesame oil can interact well with the natural rubber [because both are having a similar interaction parameter (hydrophobic−hydrophobic) and higher entropy effect (sunflower/sesame oil is smaller in size compared to the natural rubber)] and the chances for toxic ingredients (from the natural rubber) leaching are high. However, the performed in vivo experiments clearly show that both NR latex- and FLG-C-incorporated NR latex thin film nanocomposites have no clinical sign or overt toxicity, no skin irritation/sensitization, and no irritation to vaginal and penile tissues. These experiments further prove that FLG-C incorporation into NR latex does not compromise its biocompatibility.

https://dx.doi.org/10.1021/acsbiomaterials.9b01897
ACS Biomater. Sci. Eng. 2020, 6, 2007−2019

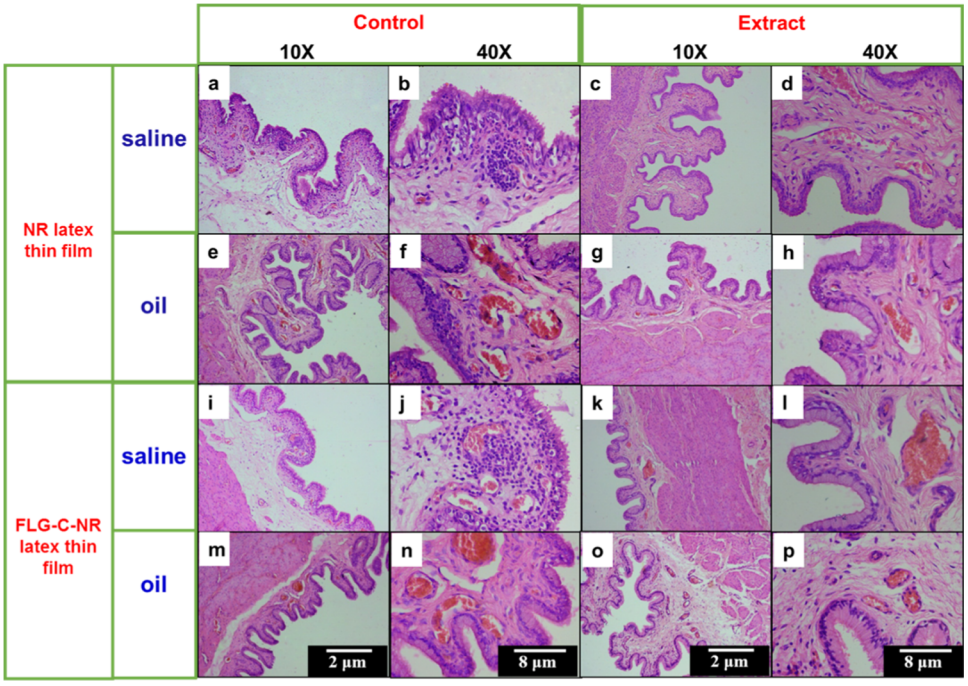

Figure 6. Representative hematoxylin and eosin-stained histopathology images of vaginal tissues of New Zealand white Rabbits.

CONCLUSIONS

For up to 48 h, no cytotoxicity is detected even for the highest concentration [1000(242) μg/mL] of FLG-C (FLG), but at longer exposure time (72 h), even the smallest content [50(12) μg/mL] provokes the cytotoxicity. Moreover, FLG-C confirms a decrease in the MMP and an increase in the ROS production at 48 h. At the same time, LDH, PI uptake, and cell cycle analysis on FLG-C are not displaying significant variation with respect to the negative control. In contrast, the performed in vitro experiments show that the extracts of NR latex and FLG-C-NR latex thin films neither decrease the cellular proliferation nor decrease/raise/change the MMP, ROS, LDH, PI uptake, and cell cycle analysis. These results suggest that FLG-C could affect the mitochondrial membrane, especially at longer exposure time (72 h), whereas the extracts of NR latex and FLG-C-NR latex are not affecting both the plasma and mitochondrial membranes. In vivo experiments such as acute systemic toxicity, skin sensitization, vaginal and penile irritation tests demonstrate that the FLG-C-NR latex thin film is biocompatible similar to the NR latex thin film.

The incorporation of FLG-C into the NR latex has increased the tensile properties (40%) without affecting the % elongation and thermal conductivity (480−980%). This would reduce the thickness [leads to reduce the weight of the product (up to 40 wt %)] and increase the consumer comfort [efficient thermal conductivity may diminish the sweating (i.e., skin-contacting rubber products) and delay the product breakdown due to the heat-induced rubber degradation]; both will be beneficial for the commercial applications. As a proof of principle, FLG-C-NR latex condom samples were prepared by the dip molding process. They showed a higher burst pressure and burst volume properties, no water leak, and similar viral passage level compared to the NR latex condoms. Therefore, these results assure that the formulated FLG can be incorporated into a range of rubber (both synthetic and natural) latexes to produce next-generation products such as condoms, gloves, cervical spacers, catheter, and other biomedical devices that come in contact with the skin and mucosal membranes such as penile and vagina.

ASSOCIATED CONTENT

Supporting Information

The Supporting Information is available free of charge at https://pubs.acs.org/doi/10.1021/acsbiomaterials.9b01897.

Data for materials characterization, in vitro and in vivo analyses; physical appearance of NR latex and FLG-C-NR latex thin film extracts used in acute systematic toxicity studies; representative photographs taken during intraperitoneal and intravenous injection for acute systematic toxicity; and representative images taken during skin sensitization experiments of NR latex/FLG-C-NR latex thin films (PDF)

AUTHOR INFORMATION

Corresponding Author

Lakshminarayanan Ragupathy − *Corporate R&D Center, HLL Lifecare Limited, Thiruvananthapuram 695017, India;* orcid.org/0000-0003-2708-2766; Email: laks@lifecarehll.com, laks77@gmail.com

Authors

Thenmozhi Sukumar − *Corporate R&D Center, HLL Lifecare Limited, Thiruvananthapuram 695017, India*

Jeslin Varghese − *Corporate R&D Center, HLL Lifecare Limited, Thiruvananthapuram 695017, India*

Kiran S − *Corporate R&D Center, HLL Lifecare Limited, Thiruvananthapuram 695017, India*

Suja Bhargavan − *Corporate R&D Center, HLL Lifecare Limited, Thiruvananthapuram 695017, India*

Parvathy Jayasree − *Corporate R&D Center, HLL Lifecare Limited, Thiruvananthapuram 695017, India*

Vemparthan Suvekbala − *Corporate R&D Center, HLL Lifecare Limited, Thiruvananthapuram 695017, India*

https://dx.doi.org/10.1021/acsbiomaterials.9b01897
ACS Biomater. Sci. Eng. 2020, 6, 2007−2019

Kumaran Alaganandam − *Corporate R&D Center, HLL Lifecare Limited, Thiruvananthapuram 695017, India*

Complete contact information is available at: https://pubs.acs.org/10.1021/acsbiomaterials.9b01897

Notes

The authors declare no competing financial interest.

■ ACKNOWLEDGMENTS

The authors thank the Bill & Melinda Gates Foundation's Grand Challenges Program for the generous financial support and HLL Lifecare Limited, Trivandrum, Kerala, India, for providing laboratory facilities and support. They are grateful to Dr. Harikumar, K.B., Rajiv Gandhi Centre for Biotechnology, for the in vitro analysis.

■ REFERENCES

(1) Wang, Y.; Li, Z.; Hu, D.; Lin, C.; Li, J.; Lin, Y. Aptamer/Graphene Oxide Nanocomplex Forin Situmolecular Probing In Living Cells. *J. Am. Chem. Soc.* **2010**, *132*, 9274−9276.

(2) Chang, H.; Tang, L.; Wang, Y.; Jiang, J.; Li, J. Graphene Fluorescence Resonance Energy Transfer Aptasensor For The Thrombin Detection. *Anal. Chem.* **2010**, *82*, 2341−2346.

(3) Bitounis, D.; Ali-Boucetta, H.; Hong, B.; Min, D.; Kostarelos, K. Prospects and Challenges of Graphene in Biomedical Applications. *Adv. Mater.* **2013**, *25*, 2258−2268.

(4) Gollavelli, G.; Ling, Y. Multi-Functional Graphene as an In Vitro and In Vivo Imaging Probe. *Biomaterials* **2012**, *33*, 2532−2545.

(5) Liu, Z.; Robinson, J.; Sun, X.; Dai, H. Pegylated Nanographene Oxide for Delivery of Water-Insoluble Cancer Drugs. *J. Am. Chem. Soc.* **2008**, *130*, 10876−10877.

(6) Ma, X.; Qu, Q.; Zhao, Y.; Luo, Z.; Zhao, Y.; Ng, K.; Zhao, Y. Graphene Oxide Wrapped Gold Nanoparticles For Intracellular Raman Imaging And Drug Delivery. *J. Mater. Chem. B* **2013**, *1*, 6495.

(7) Yang, K.; Zhang, S.; Zhang, G.; Sun, X.; Lee, S.; Liu, Z. Graphene in Mice: Ultrahigh In Vivo Tumor Uptake and Efficient Photothermal Therapy. *Nano Lett.* **2010**, *10*, 3318−3323.

(8) Pinto, A. M.; Gonçalves, I.; Magalhães, F. Graphene-Based Materials Biocompatibility: A Review. *Colloids Surf., B* **2013**, *111*, 188−202.

(9) Zhang, L.; Xia, J.; Zhao, Q.; Liu, L.; Zhang, Z. Functional Graphene Oxide As A Nanocarrier For Controlled Loading And Targeted Delivery Of Mixed Anticancer Drugs. *Small* **2010**, *6*, 537−544.

(10) Wu, X.; Ding, S.; Lin, K.; Su, J. A Review on the Biocompatibility and Potential Applications of Graphene in Inducing Cell Differentiation and Tissue Regeneration. *J. Mater. Chem. B* **2017**, *5*, 3084−3102.

(11) Pelin, M.; Fusco, L.; León, V.; Martín, C.; Criado, A.; Sosa, S.; Vázquez, E.; Tubaro, A.; Prato, M. Differential Cytotoxic Effects Of Graphene And Graphene Oxide On Skin Keratinocytes. *Sci. Rep.* **2017**, *7*, No. 40572.

(12) Baek, J.; Jeon, I.; Baek, J. Edge-Iodine/Sulfonic Acid-Functionalized Graphene Nanoplatelets as Efficient Electrocatalysts for Oxygen Reduction Reaction. *J. Mater. Chem. A* **2014**, *2*, 8690−8695.

(13) Jeon, I. Y..; Choi, H.; Jung, S.; Seo, J.; Kim, M.; Dai, L.; Baek, J. Large-Scale Production Of Edge-Selectively Functionalized Graphene Nanoplatelets Via Ball Milling And Their Use As Metal-Free Electrocatalysts For Oxygen Reduction Reaction. *J. Am. Chem. Soc.* **2013**, *135*, 1386−1393.

(14) Edwards, R. S.; Coleman, K. Graphene synthesis: relationship to applications. *Nanoscale* **2013**, *5*, 38−51.

(15) León, V.; Rodriguez, A.; Prieto, P.; Prato, M.; Vázquez, E. Exfoliation of Graphite with Triazine Derivatives under Ball-Milling Conditions: Preparation of Few-Layer Graphene via Selective Noncovalent Interactions. *ACS Nano* **2014**, *8*, 563−571.

(16) Stoller, M. D.; Park, S.; Zhu, Y.; An, J.; Ruoff, R. Graphene-Based Ultracapacitors. *Nano Lett.* **2008**, *8*, 3498−3502.

(17) Jiang, H. Chemical Preparation of Graphene-Based Nanomaterials and Their Applications in Chemical and Biological Sensors. *Small* **2011**, *7*, 2413−2427.

(18) Guo, S.; Dong, S. Graphene Nanosheet: Synthesis, Molecular Engineering, Thin Film, Hybrids, and Energy and Analytical Applications. *Chem. Soc. Rev.* **2011**, *40*, 2644.

(19) Castro Neto, A.; Guinea, F.; Peres, N.; Novoselov, K.; Geim, A. The Electronic Properties of Graphene. *Rev. Mod. Phys.* **2009**, *81*, 109−162.

(20) Balandin, A. A.; Ghosh, S.; Bao, W.; Calizo, I.; Teweldebrhan, D.; Miao, F.; Lau, C. Superior Thermal Conductivity of Single-Layer Graphene. *Nano Lett.* **2008**, *8*, 902−907.

(21) Lee, C.; Wei, X.; Kysar, J.; Hone, J. Measurement of the Elastic Properties and Intrinsic Strength of Monolayer Graphene. *Science* **2008**, *321*, 385−388.

(22) Kenry; Lee, W.; Loh, K.; Lim, C. When Stem Cells Meet Graphene: Opportunities And Challenges In Regenerative Medicine. *Biomaterials* **2018**, *155*, 236−250.

(23) Pinto, A. M.; Gonçalves, I.; Magalhães, F. Graphene-Based Materials Biocompatibility: A Review. *Colloids Surf., B* **2013**, *111*, 188−202.

(24) Bitounis, D.; Ali-Boucetta, H.; Hong, B.; Min, D.; Kostarelos, K. Prospects and Challenges of Graphene in Biomedical Applications. *Adv. Mater.* **2013**, *25*, 2258−2268.

(25) Syama, S.; Mohanan, P. Safety and Biocompatibility of Graphene: A New Generation Nanomaterial for Biomedical Application. *Int. J. Biol. Macromol.* **2016**, *86*, 546−555.

(26) Gollavelli, G.; Ling, Y. Multi-Functional Graphene as an In Vitro and In Vivo Imaging Probe. *Biomaterials* **2012**, *33*, 2532−2545.

(27) Liao, K. H.; Lin, Y.; Macosko, C.; Haynes, C. Cytotoxicity of Graphene Oxide and Graphene in Human Erythrocytes and Skin Fibroblasts. *ACS Appl. Mater. Interfaces* **2011**, *3*, 2607−2615.

(28) Fan, H.; Wang, L.; Zhao, K.; Li, N.; Shi, Z.; Ge, Z.; Jin, Z. Fabrication, Mechanical Properties, And Biocompatibility Of Graphene-Reinforced Chitosan Composites. *Biomacromolecules* **2010**, *11*, 2345−2351.

(29) Lahiri, D.; Dua, R.; Zhang, C.; de Socarraz-Novoa, I.; Bhat, A.; Ramaswamy, S.; Agarwal, A. Graphene Nanoplatelet-Induced Strengthening Of Ultrahigh Molecular Weight Polyethylene And Biocompatibility In Vitro. *ACS Appl. Mater. Interfaces* **2012**, *4*, 2234−2241.

(30) Sasidharan, A.; Swaroop, S.; Koduri, C.; Girish, C.; Chandran, P.; Panchakarla, L.; Somasundaram, V.; Gowd, G.; Nair, S.; Koyakutty, M. Comparative In Vivo Toxicity, Organ Biodistribution And Immune Response Of Pristine, Carboxylated And Pegylated Few-Layer Graphene Sheets In Swiss Albino Mice: A Three Month Study. *Carbon* **2015**, *95*, 511−524.

(31) Chen, G. Y.; Pang, D.; Hwang, S.; Tuan, H.; Hu, Y. A Graphene-Based Platform for Induced Pluripotent Stem Cells Culture and Differentiation. *Biomaterials* **2012**, *33*, 418−427.

(32) Li, N.; Zhang, Q.; Gao, S.; Song, Q.; Huang, R.; Wang, L.; Liu, L.; Dai, J.; Tang, M.; Cheng, G.; Three-Dimensional Graphene. Foam As A Biocompatible And Conductive Scaffold For Neural Stem Cells. *Sci. Rep.* **2013**, *3*, No. 1604.

(33) Crowder, S. W.; Prasai, D.; Rath, R.; Balikov, D.; Bae, H.; Bolotin, K.; Sung, H. Three-Dimensional Graphene Foams Promote Osteogenic Differentiation Of Human Mesenchymal Stem Cells. *Nanoscale* **2013**, *5*, 4171.

(34) Kim, J.; Choi, K.; Kim, Y.; Lim, K.; Seonwoo, H.; Park, Y.; Kim, D.; Choung, P.; Cho, C.; Kim, S.; et al. Bioactive Effects Of Graphene Oxide Cell Culture Substratum On Structure And Function Of Human Adipose-Derived Stem Cells. *J. Biomed. Mater. Res., Part A* **2013**, *101*, 3520−3530.

(35) Lalwani, G.; D'Agati, M.; Khan, A.; Sitharaman, B. Toxicology of Graphene-Based Nanomaterials. *Adv. Drug Delivery Rev.* **2016**, *105*, 109−144.

(36) Sasidharan, A.; Panchakarla, L.; Chandran, P.; Menon, D.; Nair, S.; Rao, C.; Koyakutty, M. Differential Nano-Bio Interactions And Toxicity Effects Of Pristine Versus Functionalized Graphene. *Nanoscale* **2011**, *3*, 2461.
(37) Khan, M.; Tahir, M.; Adil, S.; Khan, H.; Siddiqui, M.; Al-warthan, A.; Tremel, W. Graphene Based Metal And Metal Oxide Nanocomposites: Synthesis, Properties And Their Applications. *J. Mater. Chem. A* **2015**, *3*, 18753−18808.
(38) Dreyer, D.; Park, S.; Bielawski, C.; Ruoff, R. The Chemistry of Graphene Oxide. *Chem. Soc. Rev.* **2010**, *39*, 228−240.
(39) Akhavan, O. Graphene Scaffolds In Progressive Nano-technology/Stem Cell-Based Tissue Engineering of the Nervous System. *J. Mater. Chem. B* **2016**, *4*, 3169−3190.
(40) Wang, Y.; Lee, W.; Manga, K.; Ang, P.; Lu, J.; Liu, Y.; Lim, C.; Loh, K. Fluorinated Graphene For Promoting Neuro-Induction Of Stem Cells. *Adv. Mater.* **2012**, *24*, 4285−4290.
(41) Li, Y.; Feng, L.; Shi, X.; Wang, X.; Yang, Y.; Yang, K.; Liu, T.; Yang, G.; Liu, Z. Surface Coating-Dependent Cytotoxicity And Degradation Of Graphene Derivatives: Towards The Design Of Non-Toxic, Degradable Nano-Graphene. *Small* **2014**, *10*, 1544−1554.
(42) Mullick Chowdhury, S.; Lalwani, G.; Zhang, K.; Yang, J.; Neville, K.; Sitharaman, B. Cell Specific Cytotoxicity And Uptake Of Graphene Nanoribbons. *Biomaterials* **2013**, *34*, 283−293.
(43) George, G.; Sisupal, S.; Tomy, T.; Pottammal, B.; Kumaran, A.; Suvekbala, V.; Gopimohan, R.; Sivaram, S.; Ragupathy, L. Thermally Conductive Thin Films Derived From Defect Free Graphene-Natural Rubber Latex Nanocomposite: Preparation And Properties. *Carbon* **2017**, *119*, 527−534.
(44) George, G.; Sisupal, S.; Tomy, T.; Kumaran, A.; Vadivelu, P.; Suvekbala, V.; Sivaram, S.; Ragupathy, L. Facile, Environmentally Benign And Scalable Approach To Produce Pristine Few Layers Graphene Suitable For Preparing Biocompatible Polymer Nano-composites. *Sci. Rep.* **2018**, *8*, No. 11228.
(45) Sasidharan, A.; Swaroop, S.; Chandran, P.; Nair, S.; Koyakutty, M. Cellular and Molecular Mechanistic Insight into the DNA-Damaging Potential of Few-Layer Graphene in Human Primary Endothelial Cells. *Nanomedicine* **2016**, *12*, 1347−1355.
(46) Di Cristo, L.; Mc Carthy, S.; Paton, K.; Movia, D.; Prina-Mello, A. Interplay Between Oxidative Stress And Endoplasmic Reticulum Stress Mediated-Autophagy In Unfunctionalised Few-Layer Graphene-Exposed Macrophages. *2D Mater.* **2018**, *5*, No. 045033.
(47) Frontiñán-Rubio, J.; Gómez, M.; Martín, C.; González-Domínguez, J.; Durán-Prado, M.; Vázquez, E. Differential Effects Of Graphene Materials On The Metabolism And Function Of Human Skin Cells. *Nanoscale* **2018**, *10*, 11604−11615.
(48) Pelin, M.; Fusco, L.; Martín, C.; Sosa, S.; Frontiñán-Rubio, J.; González-Domínguez, J.; Durán-Prado, M.; Vázquez, E.; Prato, M.; Tubaro, A. Graphene And Graphene Oxide Induce ROS Production In Human Hacat Skin Keratinocytes: The Role Of Xanthine Oxidase And NADH Dehydrogenase. *Nanoscale* **2018**, *10*, 11820−11830.
(49) James, S.; Aparna, J. S.; Paul, A. M.; Lankadasari, M. B.; Mohammed, S.; Binu, V. S.; Santhoshkumar, T. R.; Reshmi, G.; Harikumar, K. B. Cardamonin inhibits colonic neoplasia through modulation of MicroRNA expression. *Sci. Rep.* **2017**, *7*, 13495.
(50) León, V.; Quintana, M.; Herrero, M. A.; Fierro, J. L. G.; de la Hoz, A.; Prato, M.; Vazquez, E. Few-layer graphee from ball-milling of graphite with melamine. *Chem. Commun.* **2011**, *47*, 10936−10938.
(51) Mathew, A. P.; Packirisamy, S.; Thomas, S. Studies on the thermal stability of natural rubber/polystyrene interpenetrating polymer networks:Thermogravimetric analysis. *Polym. Degrad. Stab.* **2001**, *72*, 423−439.
(52) Yan, K.; Peng, H.; Zhou, Y.; Li, H.; Liu, Z. Formation of bilayer bernal Graphene: layer-by-layer epitaxy via chemical vapor deposition. *Nano Lett.* **2011**, *11*, 1106−1110.
(53) Ferrari, A. C.; Meyer, J. C.; Scardaci, V.; Casiraghi, C.; Lazzeri, M.; Mauri, F.; Piscanec, S.; Jiang, D.; Novoselov, K. S.; Roth, S.; Geim, A. K. Raman spectrum of Graphene and Graphene layers. *Phys. Rev. Lett.* **2006**, *97*, No. 187401.
(54) Yoon, D.; Moon, H.; Cheong, H.; Choi, J.; Choi, J.; Park, B. Variations in the raman spectrum as a function of the number of Graphene layers. *J. Korean Phys. Soc.* **2009**, *55*, 1299−1303.
(55) Lytle, C. D.; Routson, L. B.; Cyr, W. H. A Simple Method To Test Condoms for Penetration by Viruses. *Appl. Environ. Microbiol.* **1992**, *58*, 3180−3182.
(56) Luo, L.; Xu, L.; Zhao, H. Biosynthesis of Reduced Graphene Oxide and its In-Vitro Cytotoxicity against Cervical Cancer (HeLa) Cell Lines. *Mater. Sci. Eng., C* **2017**, *78*, 198−202.
(57) Zhang, Q.; Liu, X.; Meng, H.; Liu, S.; Zhang, C. Reduction Pathway-Dependent Cytotoxicity of Reduced Graphene Oxide. *Environ. Sci.: Nano* **2018**, *5*, 1361−1371.
(58) Akhavan, O.; Ghaderi, E.; Akhavan, A. Size-Dependent Genotoxicity of Graphene Nanoplatelets in Human Stem Cells. *Biomaterials* **2012**, *33*, 8017−8025.

https://dx.doi.org/10.1021/acsbiomaterials.9b01897
ACS Biomater. Sci. Eng. 2020, 6, 2007−2019